COMBUSTION SYNTHESIS OF $NiCo_2O_4$ HOLE TRANSPORT LAYER FOR PEROVSKITE SOLAR CELLS

Ioannis T. Papadas[1]*, Apostolos Ioakeimidis[1], Gerasimos S. Armatas[2], Stelios A. Choulis[1]*

[1] Molecular Electronics and Photonics Research Unit, Department of Mechanical Engineering and Materials Science and Engineering, Cyprus University of Technology, Limassol, Cyprus.

[2] Department of Materials Science and Technology, University of Crete, Heraklion, Greece.

(* ioannis.papadas@cut.ac.cy, stelios.choulis@cut.ac.cy)

ABSTRACT

In the present study, we report the synthesis and characterization of a low-temperature solution-processable monodispersed nickel cobaltite ($NiCo_2O_4$) nanoparticles via a combustion method using tartaric acid as fuel and demonstrate its performance as hole transport layer (HTL) for Perovskite Solar Cells (PVSCs). We show that the combustion synthesis of spinel $NiCo_2O_4$ using tartaric acid as fuel can be used to control the NPs size and provide smooth, compact and homogeneous HTLs. The $NiCo_2O_4$ HTLs processed by bladed coating and for the optimized thickness show appropriate hole carrier selectivity and negligible PVSCs J-V hysterics. As a result, the inverted (p-i-n) structure of PVSCs with $NiCo_2O_4$ HTLs showed reliable performance and power conversion efficiency values in the range of 15.5 %.

INTRODUCTION

Over the last couple of years perovskite solar cells have been amongst the most prominent photovoltaic (PV) technologies by showing great advancement in their power conversion efficiency (PCE) from 3.8 to 22.7%.[1–5] This advancement and generally the attractiveness of perovskite solar cells as a novel research field is a result of several features such as high carrier mobility, long carrier diffusion length, high absorption coefficient, tunable band gap and low exciton binding energy.[6–9] These features allow perovskite-based solar cells to reach high PCE even when processed from solution at low temperatures. For the inverted (p-i-n-type) perovskite solar cells, poly(3,4-ethylenedioxythiophene): poly(styrenesulfonate) (PEDOT:PSS) is commonly used as a hole transport layer (HTL), followed by the perovskite layer and an n-type carrier selective contact. PEDOT:PSS is an efficient and cost-effective HTL due to its facile processing, good electrical conductivity and transparency. On the other hand, the hydroscopicity and low open circuit voltage (Voc) values obtained when applied as a HTL in PVSCs limits performance.[10,11] Recently, p-type metal oxides, such as NiO, V_2O_5, CuSCN and CuO, have been introduced into perovskite solar cells (PVSCs) as HTLs. Inorganic p-type semiconductor materials have the advantages of improved hole selectivity and Voc values, showing promising prospects as HTLs in perovskite solar cells.[12,13]

The combustion technique appears to be versatile and effective for the synthesis of high crystallinity solution-processed metal oxides thin films using low temperature. Since it is an exothermic process, with a high heat release rate, the need for high temperatures is avoided and the production of high purity nanoparticles is achieved. For the production of metal oxides, liquid phase combustion synthesis has proven to be the most suitable, where usually metal salts (for instance nitrates) serve as oxidizers dissolved in saturated aqueous or alcoholic solutions in combination with organic fuels (e.g. urea, glycine, citric acid and others). Upon heating gelation occurs and then combustion process starts resulting in the synthesis of the corresponding metal oxide.[14,15]

Nickel cobaltite ($NiCo_2O_4$) is a p-type transparent conductive oxide (TCO) semiconductor, with a relatively wide optical band gap (~2.1 - 2.4 eV), deep-lying valence band (VB of 5.3 eV) that matches well with the VB of $CH_3NH_3PbI_3$ and a much better conductivity than NiO and Co_3O_4 (at least two orders of magnitude higher). These characteristics render $NiCo_2O_4$ one of the most promising electronic materials for optoelectronic applications. These attractive features make $NiCo_2O_4$ an appropriate candidate material for introduction as hole transport layer in PVSCs to

achieve high-performance photovoltaic devices. Various synthetic routes such as hydrothermal, co-precipitation and thermal decomposition of the precursors such as hydroxide nitrates[16,17] have been developed for the synthesis of $NiCo_2O_4$. However, the production of high purity and monodispersed nanoparticles with the above mentioned synthesis approaches at low temperatures has not been completely achieved.

In this work, we present a one-step synthesis of low-temperature solution-processable nickel cobaltite ($NiCo_2O_4$) via combustion chemistry proposing for the first time tartaric acid as a fuel and nitrate as an oxidizer agent. $NiCo_2O_4$ nanoparticles (NPs) with an average size of ~4 nm and narrow particle-size distribution were prepared using a cost-effective, low-temperature combustion method calcinated at (250 - 300 ^oC) for 4 hour. These nanoparticles enable the formation of compact, smooth and high electrically conductive thin film, which were utilized, for the first time, as HTLs in a solution processed perovskite solar cell (PVSC). The corresponding PVSC exhibits a high FF = 80 % and a power conversions efficiency of 15.5 %.

EXPERIMENTAL SECTION

Synthesis of $NiCo_2O_4$ NPs films: For the combustion synthesis of $NiCo_2O_4$ NPs, 0.5 mmol $Ni(NO_3)_2.6H_2O$, 1 mmol $Co(NO_3)_2.6H_2O$ and tartaric acid were mixed in the 15 ml 2-methoxy ethanol solution. After 150 uL HNO_3 (69% wt HNO_3) were added slowly into the mixture, and the solution stirred up to almost complete homogeneity. The whole solution were allowed under stirring for 30 min at 60 ^oC. The ratio of the total metal nitrates and tartaric acid was 1. Thereafter, the violet colored solution were used for the combustion synthesis of the $NiCo_2O_4$ nanoparticles on the various substrates. Doctor blade technique were applied for the fabrication of the precursor films on the various substrates. The resulting light violet colored films were dried at 100 °C for 30 min, and used as a precursor for the combustion synthesis of $NiCo_2O_4$ NPs. Subsequently the obtained films were heated at different temperatures (200 °C, 250 °C and 300 °C) in air for 4 h in a preheated oven to complete the combustion process and then left to cool down at room temperature.

Device fabrication: The inverted solar cells under study was ITO/$NiCo_2O_4$-NPs/$CH_3NH_3PbI_3$/PC[70]BM/Al. ITO substrates were sonicated in acetone and subsequently in isopropanol for 10 min and heated at 100 ^oC on a hot plate 10 min before use. The perovskite solution was prepared 30 min prior spin coating by mixing $Pb(CH_3CO_2)_2.3H_2O$:Methylamonium iodide (1:3) at 36 %wt in DMF with the addition of 1.5 % mole of methylamonium bromide (MABr).[18] The precursor was filtered with 0.1 μm PTFE filters. The perovskite precursor solution was deposited on the HTLs by static spin coating at 4000 rpm for 60 seconds and annealed for 5 minutes at 85 ^oC, resulting in a film with a thickness of ~230 nm. The PC[70]BM solution, 20 mg ml^{-1} in chlorobenzene, was dynamically spin coated on the perovskite layer at 1000 rpm for 30 sec. Finally, 100 nm Al layers were thermally evaporated through a shadow mask to finalize the devices giving an active area of 0.9 mm^2. Encapsulation was applied directly after evaporation in the glove box using a glass coverslip and an Ossila E131 encapsulation epoxy resin activated by 365 nm UV-irradiation.

Characterization: Thermogravimetric (TGA) and Differential Thermal Analysis (DTA) were performed on a Shimadzu Simultaneous DTA-TG system (DTG-60H). Thermal analysis was conducted from 40 to 600 ^oC in air atmosphere (200 mL min^{-1} flow rate) with a heating rate of 10 ^oC min^{-1}. X-ray diffraction (XRD) patterns were collected on a PANanalytical X´pert Pro MPD powder diffractometer (40 kV, 45 mA) using Cu Kα radiation (λ=1.5418 Å). Transmission electron microscope (TEM) images and electron diffraction patterns were recorded on a JEOL JEM-2100 microscope with an acceleration voltage of 200 kV. The samples were first gently ground, suspended in ethanol and then picked up on a carbon-coated Cu grid. The thickness of the films were measured with a Veeco Dektak 150 profilometer. The current density-voltage (J-V) characteristics were characterized with a Botest LIV Functionality Test System. Both forward and reverse scans were measured with 10 mV voltage

steps and 40 msec of delay time. For illumination, a calibrated Newport Solar simulator equipped with a Xe lamp was used, providing an AM1.5G spectrum at 100 mW/cm^2 as measured by a certified oriel 91150V calibration cell. A shadow mask was attached to each device prior to measurements to accurately define the corresponding device area. Electrical conductivity measurements were performed using a four-point microposition probe, Jandel MODEL RM3000.

RESULTS AND DISCUSSION

The combustion reaction of the Ni(II)/Co(III)-tartaric complexes was monitored by differential scanning calorimetry (DSC) and thermogravimetric analysis (TGA), applying a heating rate of 10 ^{o}C/min in air. As shown in Figure 1, the reaction exhibits an intense exothermic peak at ≈260 °C in the DSC curve, which coincides well with the abrupt mass loss (at ≈250 °C) observed in TGA curve. This implies that the formation of $NiCo_2O_4$ NPs via such combustion method can effectively proceed at this temperature.

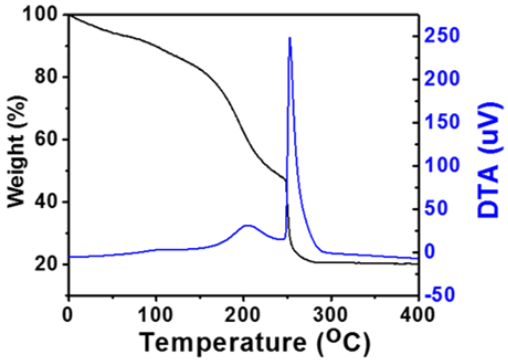

Figure 1. *TGA and DTA profiles of the as-prepared $NiCo_2O_4$ via combustion process.*

In order to crystallize the as-synthesized films to spinel phase, 4 hour of heating was applied at different temperatures, i.e. 200, 250 and 300 ^{o}C, and the XRD results of the obtained materials are shown in Figure 2a. The XRD patterns of the materials calcined at 250 and 300 ^{o}C correspond to the spinel phase of $NiCo_2O_4$, although with a larger grain composition for the sample treated at 300 ^{o}C, as indicated by the narrow full width of half-maximum (FWHM) of XRD peaks. The angular position of the diffraction peaks matches well with standard XRD pattern of cubic spinel $NiCo_2O_4$ with JCPDS card no 20–0781. The average grain of the $NiCo_2O_4$ NPs was estimated from the diffraction peak (220) by using the Scherrer's equation and was found to be ~3.5 nm for the sample annealed at 250 ^{o}C and ~5 nm for the sample annealed at 300 ^{o}C. In contrast, the XRD pattern of the material obtained after 200 °C heat treatment showed no diffraction peaks, indicating the formation of an amorphous structure.

Figure 2b displays a typical TEM image of the $NiCo_2O_4$ NPs synthesized at 250 ^{o}C. It can be seen that this material is composed of individual NPs with an average diameter of 4±1.3 nm, which is very close to the grain size calculated from XRD patterns. The high-resolution (HRTEM) image shown in Figure 2c reveals that the $NiCo_2O_4$ NPs possess a single-phase spinel structure with high crystallinity; combined with XRD results, the observed lattice fringes with interplanar distances ~2.4 Å and ~2.8 Å can be assigned to the (331) and (220) crystal planes of spinel $NiCo_2O_4$, respectively. The crystal structure of the $NiCo_2O_4$ NPs was further studied by selected-area electron diffraction (SAED). The SAED pattern taken from a small area of the $NiCo_2O_4$ NP aggregates (Figure 2d) shows a series of Debye-Scherrer diffraction rings, which can be assigned to the spinel phase of $NiCo_2O_4$. No other crystal phases were observed by means of electron diffraction.

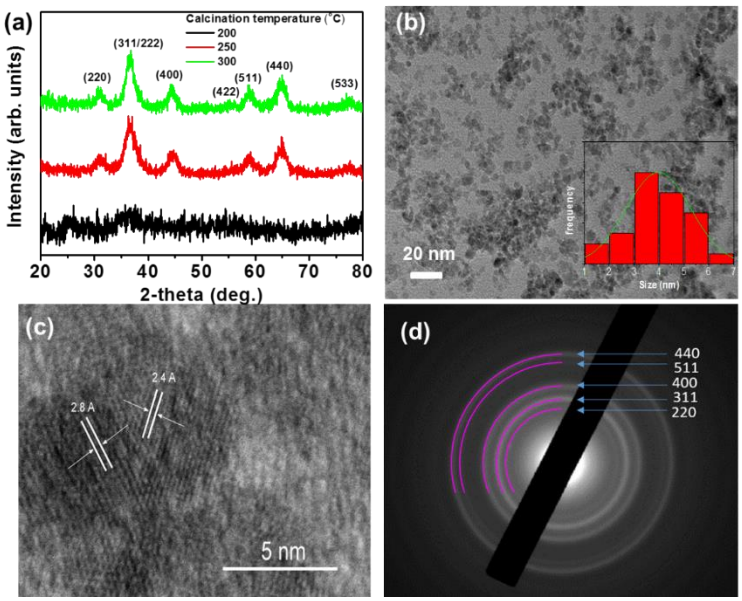

Figure 2. *(a) XRD patterns of $NiCo_2O_4$ NPs at 200 °C (black), 250 °C (red), 300 °C (green solid line) combustion temperatures. (b) Representative TEM image (inset: particle size distribution plot of the $NiCo_2O_4$ NPs at 250 °C, showing an average diameter of 4 ± 1.3 nm), (c) high-resolution TEM and (d) SAED pattern of the as-synthesized $NiCo_2O_4$ NPs obtained at 250 °C.*

The development of a low roughness HTL is a crucial parameter for the photovoltaic performance since it enables us to grow perovskite top layers with suitable interfaces. Thin films of $NiCo_2O_4$ NPs were produced on top of ITO substrates using the doctor-bladying solution processed technique, applying the coating parameters as described in the Experimental Section. Furthermore, the dense $NiCo_2O_4$ NPs-based thin film exhibits an increase electrical conductivity up to 4 S/cm at room temperature, measured using four-point probe method. Additionally, to investigate the HTL thickness dependence on the performance of p-i-n PVSCs architectures, $NiCo_2O_4$ NPs HTLs with three different thicknesses, 15, 20 and 30 nm were fabricated. On top of each $NiCo_2O_4$ layer, a 230-nm-thick perovskite film was developed as described in Experimental section. To complete the devices, a PC[70]BM film was spin-coated on the perovskite active layer serving as the electron transporting layer followed by a 100-nm-thick thermally evaporated Al top-contact (Figure 3a). Figure 3b depicts the characteristic current density – voltage curves (J – V under 1 sun simulated intensity) of the PVSCs fabricated with 15, 20 and 30 nm-thick $NiCo_2O_4$ NPs layers, and the corresponding solar cell parameters are summarized in Table 1.

Table 1. *Extracted solar cell parameters from the J – V characterization of the ITO/$NiCo_2O_4$/$CH_3NH_3PbI_3$/PC[70]BM/Al devices using $NiCo_2O_4$ HTLs with different thickness.*

$NiCo_2O_4$	Jsc [mA/cm^2]	Voc [V]	FF [%]	PCE [%]
15 nm (forw.)	19.94	0.97	79.9	15.5
(rev.)	19.60	0.99	79.2	15.4
20 nm (forw.)	18.47	0.93	73.2	12.6
(rev.)	16.83	0.97	67.8	11.1
30 nm (forw.)	18.45	0.77	61.2	8.7
(rev.)	16.29	0.90	53.0	7.8

It is observed that the J-V hysteric on the forward and reverse sweep is reduced as the thickness of $NiCo_2O_4$ decreases from 30 to 15 nm, while both the Voc and fill factor (FF) increase. Concretely, for the reversed sweep the Voc was increased from 0.90 to 0.99 V and the FF from 53.0 to 79.9 %, while

the hysteresis on the power conversion efficiency (PCE) for the 15-nm-thick $NiCo_2O_4$ layer is negligible. On the other hand, the short circuit current (Jsc) showed the lowest increase (~ 8%) for a forward sweep from 18.47 to 19.94 mA/cm^2, compared to both Voc and FF. Consequently, the device consisting of a 15-nm-thick $NiCo_2O_4$ HTL exhibits a PCE as high as 15.5% for the forward sweep. The PCE of devices with thinner $NiCo_2O_4$ layers was declined (not shown here) exhibiting high leakage current due to not fully covered ITO.

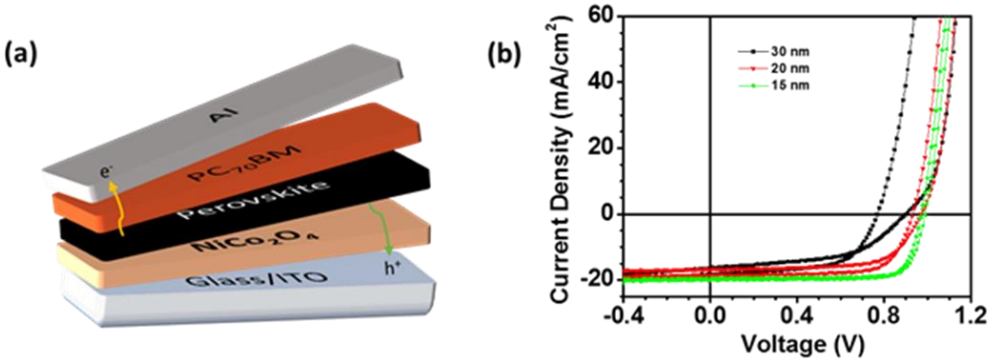

Figure 3. *(a) The structure of the p-i-n perovskite solar cells under study (ITO/$NiCo_2O_4$-NPs/$CH_3NH_3PbI_3$/PC[70]BM/Al) and (b) under 1 sun illumination conditions of the ITO/$NiCo_2O_4$-NPs/$CH_3NH_3PbI_3$ devices fabricated with $NiCo_2O_4$ with different HTL thickness (15 nm - green solid line, 20 nm - red line and 30 nm – black line).*

Importantly, improved performance reproducibility and reliability of the corresponding p-i-n perovskite solar cells achieved, when compare to our previously reported solvothermal synthesized CuO-HTL based perovskite solar cells [19] by applying the proposed combustion synthesized $NiCo_2O_4$ NPs as HTL for PVSCs. Specifically, as shown within Figure 4 the combustion synthesized $NiCo_2O_4$-HTL delivers a ~14.5 % average PCE (16 devices) with 15.5 % best performing device, while CuO-HTL based solar cells give a ~12.5 % average PCE (16 devices) with 15.3 % best performing device.[19]

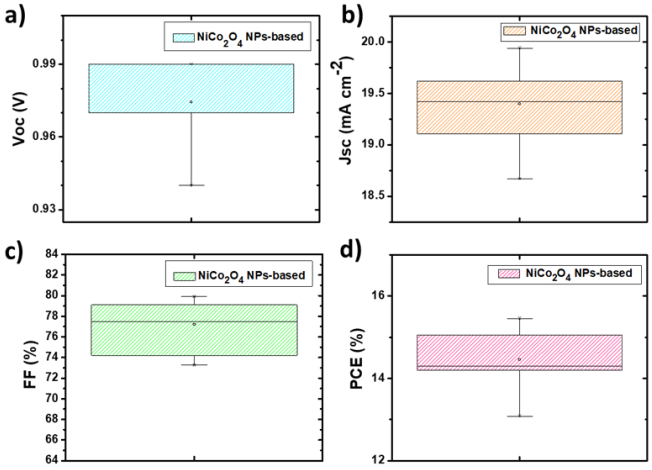

Figure 4. *Average photovoltaic parameters represented in box plots out of 16 devices of each series of p-i-n perovskite solar cells under study. $NiCo_2O_4$ HTLs-based devices with box plots, a) open circuit voltage (Voc), b) current density (Jsc), c) fill factor (FF) and d) power conversion efficiency (PCE).*

CONCLUSIONS

In conclusion, a low temperature combustion synthesis method, using tartaric acid as a fuel, was successfully developed for the first time and applied for the fabrication of compact p-type $NiCo_2O_4$ HTLs. The size of the NPs were fully controlled due to the usage of tartaric acid leading to the formation of monodispersed $NiCo_2O_4$ NPs with a diameter of ~4 nm. The combustion proceeds

under low temperature (250 °C) and reaction time (4 h) and high quality, homogeneous $NiCo_2O_4$ HLTs with high electrical conductivity (~4 $S.cm^{-1}$) and very low roughness were fabricated. The impact of $NiCo_2O_4$ HTL thicknesses on PVSCs characteristics were also investigated. The optimum HTL thickness found to be 15 nm showing enhanced charge extraction and negligible J-V hysteresis, compared to thicker films, delivering PVSCs with PCE of 15.5%. Furthermore, the results demonstrate the great potentials of applying the low-temperature combustion synthesis for fabrication of highly reproducible and reliable metal oxide NPs as transport layers in variety of solution processed optoelectronic devices.

ACKNOWLEDGEMENTS

We would like to thank Cyprus University of Technology for providing basic internal budget for the maintenance of the Molecular Electronics and Photonics Research unit and the European Research Council (ERC) under the European Union's Horizon 2020 research and innovation program (grant agreement No 647311) for funding.

REFERENCES

[1] G. Xing, N. Mathews, S. Sun, S. S. Lim, Y. M. Lam, M. Grätzel, S. Mhaisalkar, T. C. Sum. Science 342 (2013) 344-347.
[2] N. J. Jeon, J. H. Noh, W. S. Yang, Y. C. Kim, S. Ryu, J. Seo, S. Il Seok. Nature 517 (2015) 476-480.
[3] A. Kojima, K. Teshima, Y. Shirai. J Am. Chem. Soc. 131 (2009) 6050-6051.
[4] W. Sun, Y. Li, S. Ye, H. Rao, W. Yan, H. Peng, Y. Li, Z. Liu, S. Wang, Z. Chen, L. Xiao, Z. Bian, C. Huang. Nanoscale 23 (2016) 10806-10813.
[5] C. H. Chiang, Z. L. Tseng, C. G. Wu. J. Mater. Chem. A 2 (2014) 15897-15903.
[6] N. Ahn, D. Y. Son, I. H. Jang, S. M. Kang, M. Choi, N. G. Park. J. Am. Chem. Soc. 137 (2015) 8696-8699.
[7] J. H. Im, I. H. Jang, N. Pellet, M. Grätzel, N. G. Park. Nat. Nanotechnol. 9 (2014) 927-932.
[8] X. Gong, M. Li, X. B. Shi, H. Ma, Z. K. Wang, L. S. Liao. Adv. Funct. Mater. 25 (2015) 6671-6678.
[9] H. P. Zhou, Q. Chen, G. Li, S. Luo, T. B. Song, H. S. Duan, Z. R. Hong, J. B. You, Y. S. Liu, Y. Yang. Science 345 (2014) 542-546.
[10] J. H. Kim, P. W. Liang, S. T. Williams, N. Cho, C. C. Chueh, M. S. Glaz, D. S. Ginger, A. K. Y. Jen. Adv. Mater. 27 (2015) 695-701.
[11] Z. K. Wang, M. Li, D. X. Yuan, X. B. Shi, H. Ma, L. S. Liao. ACS Appl. Mater. Interfaces 7 (2015) 9645-9651.
[12] V. Shrotriya, G. Li, Y. Yao, C.-W. Chu, Y. Yang. Appl. Phys. Lett. 88 (2006) 73508-73512.
[13] M. T. Greiner, M. G. Helander, W.-M. Tang, Z.-B. Wang, J. Qiu, Z.-H. Lu. Nat. Mater. 11 (2011) 76-81.
[14] A. K. Alves, C. P. Bergmann, F. A. Berutti. Novel Synthesis and Characterization of Nanostructured Materials, Springer 1 (2013) 1-92.
[15] G. C. Pontelli, R. P. Reolon, A. K. Alves, F. A. Berutti, C. P. Bergmann. App. Catal. A 405 (2011) 79-83.
[16] J. F. Marco, J. R. Gancedo, M. Gracia, J. L. Gautier, E. Ríos, F. J. Berry. Solid St. Chem. 153 (2000) 74-81.
[17] L. Markov, K. Petrov. Reactivity of Solids 1 (1986) 319-327.
[18] L. Zhao, D. Luo, J. Wu, Q. Hu, W. Zhang, K. Chen, T. Liu, Y. Liu, Y. Zhang, F. Liu, T. P. Russell, H. J. Snaith, R. Zhu, Q. Gong. Adv. Funct. Mater. 26 (2016) 3508-3514.
[19] A. Savva, I. T. Papadas, D. Tsikritzis, G. S. Armatas, S. Kennou, S. A. Choulis. J. Mater. Chem. A 5 (2017) 20381-20389.